# Tris(2-mercaptoimidazolyl)hydroborato Cadmium Thiolate Complexes, [Tm^Bu^t]CdSAr: Thiolate Exchange at Cadmium in a Sulfur-Rich Coordination Environment

Ava Kreider-Mueller, Patrick J. Quinlivan, Jonathan S. Owen,*[ID] and Gerard Parkin*[ID]

Department of Chemistry, Columbia University, New York, New York 10027, United States

Ⓢ *Supporting Information*

ABSTRACT: A series of cadmium thiolate compounds that feature a sulfur-rich coordination environment, namely $[Tm^{Bu^t}]CdSAr$, have been synthesized by the reactions of $[Tm^{Bu^t}]CdMe$ with ArSH (Ar = C_6H_4-4-F, C_6H_4-4-Bu^t, C_6H_4-4-OMe, and C_6H_4-3-OMe). In addition, the pyridine-2-thiolate and pyridine-2-selenolate derivatives, $[Tm^{Bu^t}]CdSPy$ and $[Tm^{Bu^t}]$-CdSePy have been obtained via the respective reactions of $[Tm^{Bu^t}]$CdMe with pyridine-2-thione and pyridine-2-selone. The molecular structures of $[Tm^{Bu^t}]CdSAr$ and $[Tm^{Bu^t}]CdEPy$ (E = S or Se) have been determined by X-ray diffraction and demonstrate that, in each case, the $[CdS_4]$ motif is distorted tetrahedral and approaches a trigonal monopyramidal geometry in which the thiolate ligand adopts an equatorial position; $[Tm^{Bu^t}]CdSPy$ and $[Tm^{Bu^t}]CdSePy$, however, exhibit an additional long-range interaction with the pyridyl nitrogen atoms. The ability of the thiolate ligands to participate in exchange was probed by ^1H and ^{19}F nuclear magnetic resonance (NMR) spectroscopic studies of the reactions of $[Tm^{Bu^t}]CdSC_6H_4$-4-F with ArSH (Ar = C_6H_4-4-Bu^t or C_6H_4-4-OMe), which demonstrate that (i) exchange is facile and (ii) coordination of thiolate to cadmium is most favored for the *p*-fluorophenyl derivative. Furthermore, a two-dimensional EXSY experiment involving $[Tm^{Bu^t}]CdSC_6H_4$-4-F and 4-fluorothiophenol demonstrates that degenerate thiolate ligand exchange is also facile on the NMR time scale.
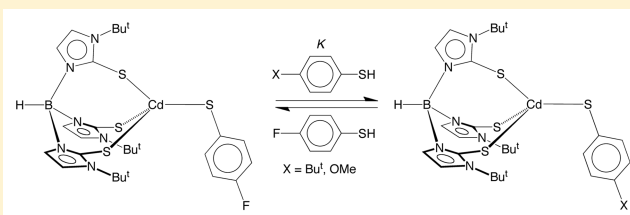
INTRODUCTION

Thiolate ligands are prevalent in the coordination chemistry of both transition and main group metals,[1] having found important applications in the fields of bioinorganic chemistry[2] and nanoscience.[3] For example, many enzymes feature metal coordination by the thiolate groups of cysteine residues,[4] as illustrated by a large variety of zinc enzymes, such as liver alcohol dehydrogenase, 5-aminolevulinate dehydratase, the Ada DNA repair protein, and zinc finger proteins.[5−7] Indeed, the first cadmium enzyme discovered likewise exhibits coordination by cysteine thiolate groups,[8] but it should be noted that such coordination is additionally associated with both (i) a mechanism of cadmium toxicity and (ii) the ability of metallothionein to protect against cadmium toxicity.[9−12] With respect to applications in nanoscience, cadmium−thiolate coordination has also been used as a means to cap cadmium chalcogenide nanoparticles.[3a,b,13] Therefore, in view of the current relevance of cadmium−thiolate interactions, we report here an investigation of thiolate exchange at cadmium in a sulfur-rich coordination environment.

RESULTS AND DISCUSSION

The tris(2-mercaptoimidazolyl)hydroborato ligand system, $[Tm^R]$ (Figure 1),[14−18] has been shown to be effective for providing an L_2X^{19} $[S_3]$ donor array for a variety of metal centers. For example, this class of ligands has been utilized for investigating zinc enzymes that have sulfur-rich active sites.[16,20−23]
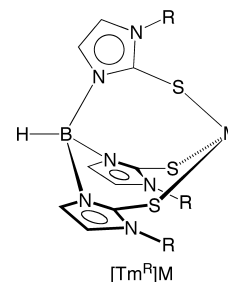
Figure 1. $[Tm^R]$ ligands in their κ^3 coordination mode.

Cadmium[24−29] and mercury[28c,29a,30,31] counterparts have also been synthesized, with the latter providing a molecular model for mercury detoxification by organomercurial lyase (*MerB*).[30a] Thiolate exchange involving the $\{[Tm^R]Cd\}$ platform, however, has received no attention, so here we report the synthesis and structures of $[Tm^{Bu^t}]CdSAr$ compounds and their exchange reactions with thiols.

Synthesis and Structural Characterization of $[Tm^{Bu^t}]$-CdSAr. Cadmium thiolate compounds of the class $[Tm^R]CdSAr$ were first synthesized by Rabinovich via the reactions of $[Tm^{p\text{-}Tol}]CdBr$ with the thallium(I) thiolate reagents, TlSAr.[28a,32]

Subsequently, we demonstrated that $[Tm^{Bu^t}]CdSAr$ derivatives could also be obtained by treatment of $[Tm^{Bu^t}]CdMe$ with ArSH (Ar = C_6H_5 or C_6H_4-4-Me).[24] Since a variety of thiols are commercially available (in contrast to TlSAr), we have used the latter method to extend the series of $[Tm^{Bu^t}]CdSAr$ derivatives (Ar = C_6H_4-4-F, C_6H_4-4-Bu^t, C_6H_4-4-OMe, or C_6H_4-3-OMe), as illustrated in Scheme 1. The molecular structures of all of the $[Tm^{Bu^t}]CdSAr$ derivatives have been determined by X-ray diffraction, as illustrated in Figures 2−5, and selected bond lengths and angles are listed in Table 1.

The coordination geometry of the cadmium center in each $[Tm^{Bu^t}]CdSAr$ derivative is distorted tetrahedral, as indicated by the deviation of the four-coordinate τ_4 and τ_δ geometry indices[33] from the idealized value of 1.00 for a tetrahedral geometry (Table 3). Specifically, the distortion is such that the structures approach a trigonal monopyramidal geometry (0.85) in which the thiolate ligand adopts an equatorial position. In this regard, the sum of the three bond angles (Σ_{S-Cd-S}) that approximate the equatorial plane [333.7−347.2° (Table 3)] is greater than the idealized tetrahedral value (328.5°).

With respect to the coordination of the thiolate ligands, the Cd−SAr bond lengths are ∼0.1 Å shorter than the average Cd−S bond lengths associated with the $[Tm^{Bu^t}]$ ligands (Table 1), which is in accord with the latter involving a dative covalent component to the bonding interaction.[34] The Cd−S−Ar bond angles exhibit little variation [103.77(9)−106.39(11)°] and are comparable to the mean value of 106.5° for structurally characterized cadmium arylthiolate compounds listed in the Cambridge Structural Database (CSD).[35] Despite the similar Cd−SAr bond lengths and Cd−S−Ar bond angles, however, the Cd−S−C$_{ipso}$−C$_{ortho}$ torsion angles (Figure 6) vary significantly (Table 2), with $[Tm^{Bu^t}]CdSC_6H_4$-4-F having the smallest Cd−S−C$_{ipso}$−C$_{ortho}$ torsion angle (2.09°) and $[Tm^{Bu^t}]CdSC_6H_4$-4-OMe having the largest torsion angle (42.81°). Of note, $[Tm^{Bu^t}]CdSC_6H_4$-4-OMe and $[Tm^{Bu^t}]CdSC_6H_4$-3-OMe have similar torsion angles, which suggests that steric effects do not have much influence in this system. Since the distance between the *ortho* hydrogen and the cadmium varies with the torsion angle, it is appropriate to consider the possibility that the small torsion angle for $[Tm^{Bu^t}]CdSC_6H_4$-4-F could reflect an agostic interaction.[36] The Cd···H distance (2.70 Å), however, is considerably longer than the sum of the covalent radii of Cd
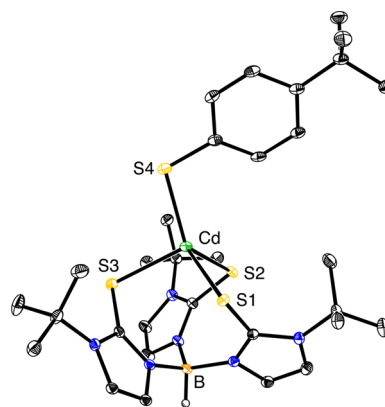

Figure 2. Molecular structure of $[Tm^{Bu^t}]CdSC_6H_4$-4-Bu^t.
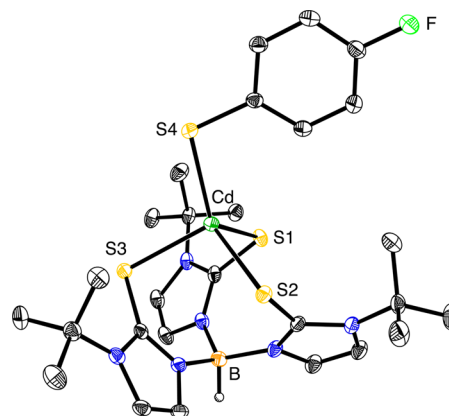
Figure 3. Molecular structure of $[Tm^{Bu^t}]CdSC_6H_4$-4-F.

and H (1.75 Å)[37] and is also longer than the Cd···H−B distance in $[\kappa^2$-$Tm^{Bu^t}]_2Cd$ (2.49 Å).[24] As such, it is not reasonable to attribute the orientation of the aryl group of $[Tm^{Bu^t}]CdSC_6H_4$-4-F to an agostic interaction, and crystal packing effects are more likely responsible for the variation of torsion angles.

Synthesis and Structural Characterization of $[Tm^{Bu^t}]$-CdSPy and $[Tm^{Bu^t}]CdSePy$. In addition to arylthiolate compounds, $[Tm^{Bu^t}]CdSAr$, we have also synthesized the
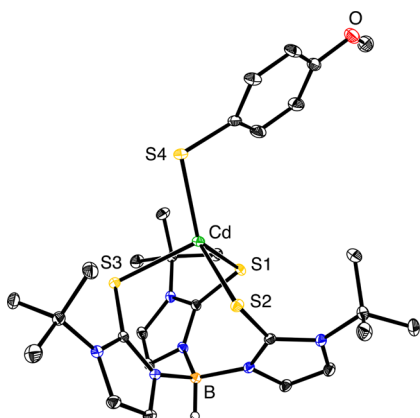
Scheme 1
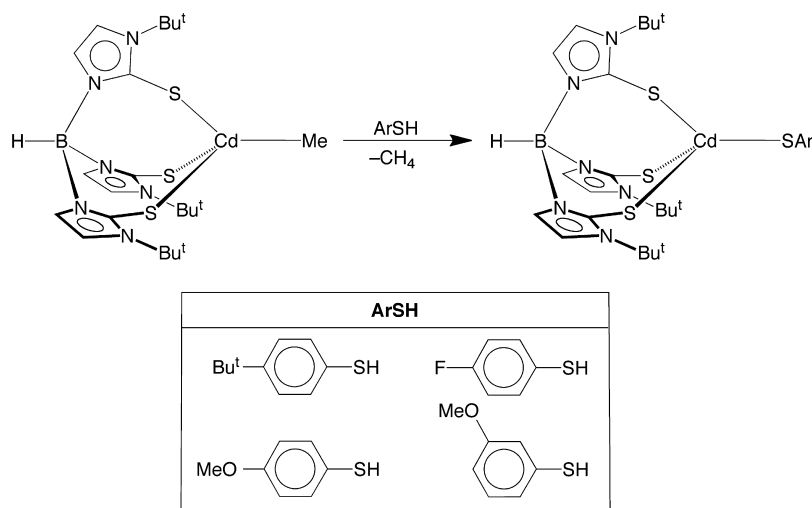
Figure 4. Molecular structure of $[\text{Tm}^{\text{Bu}^t}]\text{CdSC}_6\text{H}_4\text{-4-OMe}$.
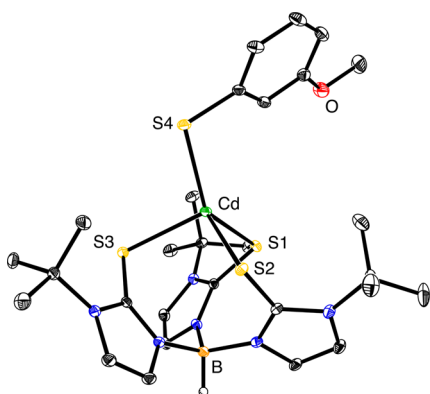

Figure 5. Molecular structure of $[\text{Tm}^{\text{Bu}^t}]\text{CdSC}_6\text{H}_4\text{-3-OMe}$.

pyridine-2-thiolate[38] counterpart, $[\text{Tm}^{\text{Bu}^t}]\text{CdSPy}$, via the reaction of $[\text{Tm}^{\text{Bu}^t}]\text{CdMe}$ with pyridine-2-thione[39] (Scheme 2). The molecular structure of $[\text{Tm}^{\text{Bu}^t}]\text{CdSPy}$ has been determined by X-ray diffraction (Figure 7), which indicates that it exists as a discrete mononuclear compound. Although a variety of metal compounds derived from 2-mercaptopyridine have been reported,[40] the formation of $[\text{Tm}^{\text{Bu}^t}]\text{CdSPy}$ is noteworthy because there is only one pyridine-2-thiolate cadmium compound listed in the CSD,[35] namely Cd(SPy)_2;[41,42] furthermore, Cd(SPy)_2 is polymeric with each sulfur bridging two cadmium atoms.

Table 2. Bond Angles and Torsion Angles Pertaining to the Thiolate Ligands of $[\text{Tm}^{\text{Bu}^t}]\text{CdSAr}$

compound	Cd–S–C$_{ipso}$ (deg)	Cd–S–C$_{ipso}$–C$_{ortho}$ (deg)
$[\text{Tm}^{\text{Bu}^t}]\text{CdSC}_6\text{H}_5$[a]	105.14(9)	15.25
$[\text{Tm}^{\text{Bu}^t}]\text{CdSC}_6\text{H}_4\text{-4-Me}$[a]	106.39(11)	31.49
$[\text{Tm}^{\text{Bu}^t}]\text{CdSC}_6\text{H}_4\text{-4-Bu}^t$	105.87(7)	19.56
$[\text{Tm}^{\text{Bu}^t}]\text{CdSC}_6\text{H}_4\text{-4-OMe}$	105.88(5)	42.81
$[\text{Tm}^{\text{Bu}^t}]\text{CdSC}_6\text{H}_4\text{-3-OMe}$	104.02(6)	38.91
$[\text{Tm}^{\text{Bu}^t}]\text{CdSC}_6\text{H}_4\text{-4-F}$	103.77(9)	2.09

[a]Data taken from ref 24.

Table 3. Four-Coordinate τ_4 and τ_δ Indices and $\Sigma_{\text{S–Cd–E}}$ Values for $[\text{Tm}^{\text{Bu}^t}]\text{CdSAr}$ and $[\text{Tm}^{\text{Bu}^t}]\text{CdEPy}$ (E = S or Se)

compound	τ_4	τ_δ	$\Sigma_{\text{S–Cd–E}}$ (deg)[b]
$[\text{Tm}^{\text{Bu}^t}]\text{CdSC}_6\text{H}_5$[a]	0.82	0.82	342.17
$[\text{Tm}^{\text{Bu}^t}]\text{CdSC}_6\text{H}_4\text{-4-Me}$[a]	0.80	0.75	333.66
$[\text{Tm}^{\text{Bu}^t}]\text{CdSC}_6\text{H}_4\text{-4-Bu}^t$	0.79	0.77	344.73
$[\text{Tm}^{\text{Bu}^t}]\text{CdSC}_6\text{H}_4\text{-4-OMe}$	0.80	0.76	347.21
$[\text{Tm}^{\text{Bu}^t}]\text{CdSC}_6\text{H}_4\text{-3-OMe}$	0.80	0.67	345.17
$[\text{Tm}^{\text{Bu}^t}]\text{CdSC}_6\text{H}_4\text{-4-F}$	0.83	0.80	341.14
$[\text{Tm}^{\text{Bu}^t}]\text{CdSPy}$	0.74[c]	0.72[c]	354.92
$[\text{Tm}^{\text{Bu}^t}]\text{CdSePy}$	0.75[c]	0.75[c]	353.62

[a]Data taken from ref 24. [b]Sum of the three angles for the atoms that approximate to trigonal planar. [c]Values assuming no Cd–N interaction.

Selected bond lengths and angles for $[\text{Tm}^{\text{Bu}^t}]\text{CdSPy}$ are summarized in Table 4, indicating that the Cd–SPy bond length [2.4946(8) Å] is comparable to the Cd–SAr bond lengths in the aforementioned $[\text{Tm}^{\text{Bu}^t}]\text{CdSAr}$ complexes (Table 1). Despite the similar Cd–S bond lengths, however, the bond angle at the thiolate sulfur [91.95(10)°] is much smaller than those of the arylthiolate compounds listed in Table 1 [103.77(9)– 106.39(11)°]. In addition to a small angle at sulfur, the Cd–S–C–N torsion angle is close to zero (0.35°), both of which indicate that the pyridine ring is oriented in a position that would maximize a Cd···N interaction. Of note, these structural features are not present in the pyridine-2-thione adduct, $[\text{Cd(SPyH)}_4]^{2+}$.[43] Specifically, the bond angles at the sulfur atoms of $[\text{Cd(SPyH)}_4]^{2+}$ (107.8° and 109.1°) are much larger than that for $[\text{Tm}^{\text{Bu}^t}]\text{CdSPy}$, as are the torsion angles (121.0° and 175.0°).

However, despite the favorable orientation of the pyridine ring of $[\text{Tm}^{\text{Bu}^t}]\text{CdSPy}$ to participate in a Cd···N interaction, the

Table 1. Selected Bond Lengths (angstroms) and Angles (degrees) for $[\text{Tm}^{\text{Bu}^t}]\text{CdSAr}$

	C$_6$H$_5$[a]	C$_6$H$_4$-4-Me[a]	C$_6$H$_4$-4-Bu^t	C$_6$H$_4$-4-OMe	C$_6$H$_4$-3-OMe	C$_6$H$_4$-4-F
Cd–S(1)	2.5784(6)	2.5680(10)	2.5597(6)	2.5576(7)	2.5537(5)	2.5621(8)
Cd–S(2)	2.5537(6)	2.5622(10)	2.5648(6)	2.5672(7)	2.5579(5)	2.5560(7)
Cd–S(3)	2.5641(6)	2.5643(10)	2.5601(7)	2.5681(7)	2.5596(5)	2.5475(7)
Cd–S(4)	2.4595(7)	2.4648(10)	2.4419(7)	2.4308(7)	2.4462(5)	2.4565(7)
Cd–$[\text{Tm}^{\text{Bu}^t}]$[b]	2.57[1]	2.565[3]	2.562[3]	2.564[6]	2.557[3]	2.555[7]
{Cd–$[\text{Tm}^{\text{Bu}^t}]$}[b]–{Cd–S(4)}	0.11	0.100	0.120	0.133	0.111	0.099
S(1)–Cd–S(2)	97.68(2)	97.56(3)	95.82(2)	99.52(2)	97.879(16)	97.54(2)
S(1)–Cd–S(3)	102.78(2)	97.61(3)	102.443(19)	98.68(2)	98.899(15)	102.95(2)
S(1)–Cd–S(4)	122.39(2)	127.83(4)	122.81(2)	126.52(2)	134.208(16)	119.87(3)
S(2)–Cd–S(3)	100.458(19)	102.72(3)	103.09(5)	99.18(2)	103.193(16)	102.49(2)
S(2)–Cd–S(4)	122.00(2)	108.27(3)	126.10(2)	121.17(2)	113.083(16)	123.73(3)
S(3)–Cd–S(4)	108.12(2)	118.68(3)	103.152(19)	106.52(2)	105.421(17)	107.39(2)
Cd–S(4)–C(Ar)	105.14(9)	106.39(11)	105.87(7)	105.88(5)	104.02(6)	103.77(9)

[a]Data taken from ref 24. [b]Average value of the Cd–S bond lengths involving the $[\text{Tm}^{\text{Bu}^t}]$ ligand.
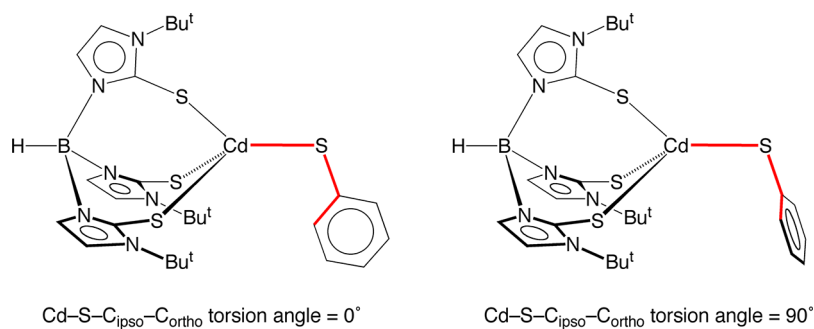
Figure 6. Cd−S−C$_{ipso}$−C$_{ortho}$ torsion angles in [Tm$^{Bu^t}$]CdSAr.

Scheme 2
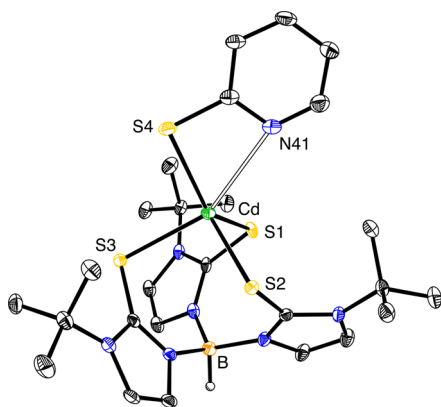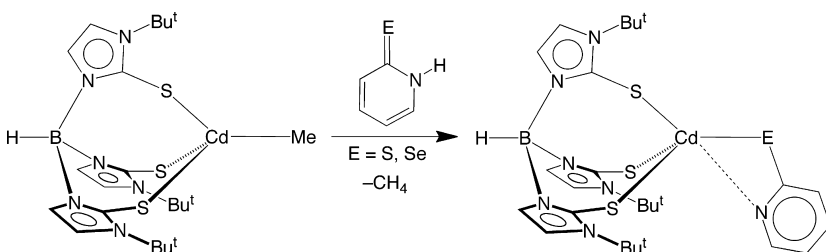
Figure 7. Molecular structure of [Tm$^{Bu^t}$]CdSPy.

Figure 8. Coordination modes for pyridine-2-thiolate ligands (only one resonance structure is shown in each case).

Table 4. Selected Bond Lengths (angstroms) and Angles (degrees) for [Tm$^{Bu^t}$]CdEPy (E = S or Se)

	[Tm$^{Bu^t}$]CdSPy	[Tm$^{Bu^t}$]CdSePy
Cd−S(1)	2.5509(7)	2.5513(6)
Cd−S(2)	2.5633(7)	2.5594(6)
Cd−S(3)	2.6438(7)	2.6361(5)
Cd−E	2.4946(8)	2.5709(4)
Cd⋯N(41)	2.766	3.000
S(1)−Cd−S(2)	99.78(2)	99.115(17)
S(1)−Cd−S(3)	99.47(2)	99.490(19)
S(2)−Cd−S(3)	97.43(2)	98.50(2)
S(1)−Cd−E	129.26(3)	127.095(17)
S(2)−Cd−E	125.88(3)	127.408(14)
S(3)−Cd−E	95.63(2)	97.125(17)
Cd−E−C$_{ipso}$	91.95(10)	93.32(5)

Cd⋯N distance of 2.766 Å is distinctly longer than the average value of 2.350 Å for structurally characterized cadmium pyridine compounds listed in the CSD.[35,44] As such, it is evident that the Cd⋯N interaction in [Tm$^{Bu^t}$]CdSPy cannot be regarded as
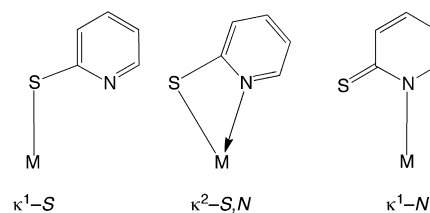
strong. Pyridine-2-thiolate ligands are known to coordinate to a single metal center via three possible coordination modes (Figure 8),[40,45] namely, κ^1-S,[46] κ^1-N,[47] and κ^2-S,N,[46a,48] so it is apparent that [Tm$^{Bu^t}$]CdSPy possesses a structure that lies on the border between κ^1-S and κ^2-S,N coordination modes.

Interestingly, even though the Cd⋯N interaction is not strong, the presence of the nitrogen does, nevertheless, have an impact on the cadmium coordination geometry. For example, one of the Cd−S bonds involving the [Tm$^{Bu^t}$] ligand is distinctly longer than the other two. Specifically, the sulfur that is approximately *trans* to the nitrogen atom [S(3)−Cd−N, 154.92°] has a Cd−S(3) bond length of 2.6438(7) Å, whereas the other two have bond lengths of 2.5509(7) and 2.5633(7) Å. For further comparison, the longest Cd−S bond length involving the [Tm$^{Bu^t}$] ligand for the thiolate compounds listed in Table 1 is 2.5784(6) Å. Neglecting the Cd⋯N interaction, the τ_4 parameter (0.74) is smaller than the values for the other [Tm$^{Bu^t}$]CdSAr compounds. As such, the cadmium center of the [CdS$_4$] moiety is approaching a trigonal monopyramidal geometry in which the longest Cd−S bond occupies the axial position. In accord with the approximate trigonal monopyramidal description for the [CdS$_4$] moiety, the PyS−Cd−S angle involving the axial sulfur of the [Tm$^{Bu^t}$] ligand [95.63(2)°] is close to 90°, whereas the corresponding value for [Tm$^{Bu^t}$]-CdSPh [108.12(2)°] is close to the tetrahedral angle. Furthermore, the sum of the three bond angles ($\Sigma_{S−Cd−S}$) that approximate the equatorial plane (354.9°) is very close to that required

for a planar arrangement (360.0°). Thus, the structure of $[Tm^{Bu^t}]CdSPy$ may be considered to be intermediate between trigonal monopyramidal $[CdS_4]$ and distorted trigonal bipyramidal $[CdS_4N]$.

By comparison to pyridine-2-thiolate compounds, their selenium counterparts have received comparatively little attention,[49−51] and there are only two structurally characterized cadmium pyridine-2-selenolate derivatives listed in the CSD, namely, $Cd(SePy)_2(tmeda)$[51b] and $Cd(SePy)_2$,[51a] of which the latter is polymeric. In this regard, we have extended this investigation to the synthesis of the selenium counterpart, $[Tm^{Bu^t}]CdSePy$, as illustrated in Scheme 2. The molecular structure of $[Tm^{Bu^t}]CdSePy$ has been determined by X-ray diffraction (Figure 9), thereby
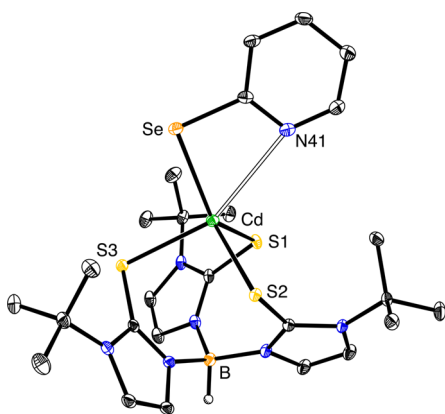
Figure 9. Molecular structure of $[Tm^{Bu^t}]CdSePy$.

demonstrating that the pyridine-2-selenolate ligand coordinates in a predominantly κ^1-*Se* manner, in contrast to the κ^2-*Se,N* coordination mode observed for $Cd(SePy)_2(tmeda)$.[51b] Specifically, whereas the Cd−Se bond length of $[Tm^{Bu^t}]CdSePy$ [2.5709(4) Å] is shorter than that of $Cd(SePy)_2(tmeda)$ [2.734(3) and 2.735(3) Å],[52] the Cd···N distance of $[Tm^{Bu^t}]$-CdSePy (3.000 Å) is much longer than those for $Cd(SePy)_2(tmeda)$ [2.399(19) and 2.40(2) Å]. Furthermore, the Cd···N distance of $[Tm^{Bu^t}]CdSePy$ is also considerably longer than that for $[Tm^{Bu^t}]$-CdSPy (2.766 Å).[53] The Cd−Se−C−N torsion angle (0.95°) is, nevertheless, close to zero, so that it is appropriately located to participate in a potential Cd···N interaction. In this regard, the Cd−S bond [2.6361(5) Å] of the $[Tm^{Bu^t}]$ ligand that is approximately *trans* to the nitrogen is distinctly longer than the other two [2.5513(6) and 2.5594(6) Å], such that the structure approaches trigonal monopyramidal ($\tau_4 = 0.75$). Furthermore, the sum of the three bond angles ($\Sigma_{S−Cd−E}$) that approximate the equatorial plane is 353.6°. Thus, even though the Cd···N distance is long, the presence of the nitrogen has an impact on the cadmium coordination geometry in a manner similar to that observed for $[Tm^{Bu^t}]CdSPy$.

Thiolate Exchange between $[Tm^{Bu^t}]CdSAr$ and Ar′SH. To evaluate the factors that influence the coordination of thiolate ligands to cadmium, we have investigated thiolate exchange reactions involving $[Tm^{Bu^t}]CdSAr$ and Ar′SH to determine which substituents promote thiolate coordination. For example, $[Tm^{Bu^t}]CdSC_6H_4$-4-F reacts rapidly with Ar′SH (Ar = C_6H_4-4-Bu^t or C_6H_4-4-OMe) to yield an equilibrium mixture comprising $[Tm^{Bu^t}]CdSC_6H_4$-4-F, $[Tm^{Bu^t}]CdSAr$, and the respective thiols (Scheme 3), as monitored by ^1H and ^{19}F nuclear magnetic resonance (NMR) spectroscopy. The derived equilibrium constants are summarized in Table 5, which illustrates that coordination of thiolate is favored for the more electron-withdrawing

fluoride substituent. This observation is in accord with our previous studies concerned with coordination of alkoxide to zinc, which shows that such coordination is also favored for electron-withdrawing substituents.[54] The thermodynamics of the cadmium thiolate exchange reactions are dictated by the differential effect of the substituent on the Cd−SAr and H−SAr bond energies. On the basis of the aforementioned zinc alkoxide study,[54] the observed thermodynamic trend can be rationalized by electron-withdrawing substituents increasing the Cd−SAr bond dissociation energies to a greater degree than the H−SAr bond dissociation energies.[55,56] Alternatively, in terms of arguments based on heterolytic bond dissociation energies, electron-withdrawing substituents weaken Cd−SAr bonds to a smaller degree than they do for H−SAr bonds.[57−59]

While the equilibrium studies described above indicate that thiolate exchange is facile on the chemical time scale, two-dimensional EXSY[60] studies involving $[Tm^{Bu^t}]CdSC_6H_4$-4-F and 4-fluorothiophenol indicate that degenerate thiolate ligand exchange is also facile on the magnetization transfer NMR time scale (Figure 10).[61] Specifically, exchange is indicated by the observation of an off-diagonal cross peak between the ^{19}F NMR spectroscopic signals for $[Tm^{Bu^t}]CdSC_6H_4$-4-F and 4-fluoro-thiophenol. The observation of thiolate exchange between $[Tm^{Bu^t}]CdSAr$ and ArSH (Ar = C_6H_4-4-F) complements the observation that exchange of thiolate ligands between zinc and cadmium centers of $[Tm^{Bu^t}]ZnSCH_2C(O)N(H)Ph$ and $[Tm^{Bu^t}]$-$CdSCH_2C(O)N(H)Ph$ is also facile on the NMR time scale.[20b,26,27]

■ CONCLUSIONS

A series of cadmium thiolate compounds that feature a sulfur-rich coordination environment, namely $[Tm^{Bu^t}]CdSAr$, have been synthesized by the reactions of $[Tm^{Bu^t}]CdMe$ with ArSH (Ar = C_6H_4-4-F, C_6H_4-4-Bu^t, C_6H_4-4-OMe, or C_6H_4-3-OMe). The molecular structures of the thiolate compounds have been determined by X-ray diffraction, which demonstrate that the coordination geometry is distorted tetrahedral and approaches a trigonal monopyramidal geometry in which the thiolate ligand adopts an equatorial position. The pyridine-2-thiolate and pyridine-2-selenolate derivatives, $[Tm^{Bu^t}]CdSPy$ and $[Tm^{Bu^t}]$-CdSePy, have also been obtained via the respective reactions of $[Tm^{Bu^t}]CdMe$ with pyridine-2-thione and pyridine-2-selone, and X-ray diffraction studies demonstrate that the nitrogen of the pyridine ring exhibits a long-range interaction with the cadmium. The ability of the thiolate ligands to participate in exchange was probed by ^1H and ^{19}F NMR spectroscopic studies of the reactions of $[Tm^{Bu^t}]CdSC_6H_4$-4-F with ArSH (Ar = C_6H_4-4-Bu^t or C_6H_4-4-OMe), which demonstrate that (i) exchange is facile and (ii) coordination of thiolate to cadmium is most favored for the *p*-fluorophenyl derivative. Furthermore, a two-dimensional EXSY experiment involving $[Tm^{Bu^t}]CdSC_6H_4$-4-F and 4-fluoro-thiophenol demonstrates that degenerate thiolate ligand exchange is also facile on the NMR time scale.

■ EXPERIMENTAL SECTION

General Considerations. All manipulations were performed by using a combination of glovebox, high-vacuum, and Schlenk techniques under a nitrogen or argon atmosphere.[62] Solvents were purified and degassed by standard procedures. NMR spectra were recorded on Bruker 300 DRX, Bruker 300 DPX, Bruker 400 Avance III, Bruker 400 Cyber-enabled Avance III, and Bruker 500 DMX spectrometers. ^1H NMR spectra are reported in parts per million relative to SiMe$_4$ (δ 0) and were referenced internally with respect to the protio solvent impurity (δ 7.16 for C_6D_5H and δ 5.32 for CHDCl$_2$).[63] ^{13}C NMR

Scheme 3
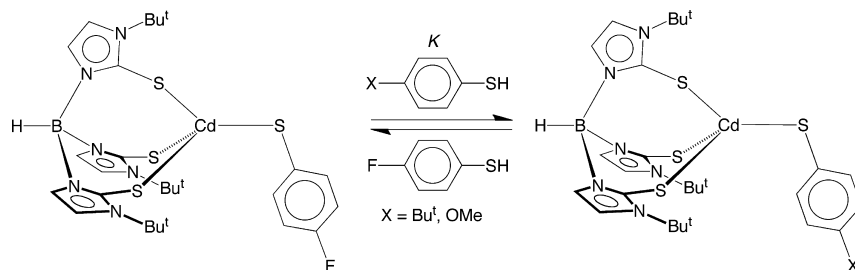
Table 5. Equilibrium Constants (K) for the Reaction of [Tm$^{Bu^t}$]CdSC$_6$H$_4$-4-F with ArSH

Ar	K
C$_6$H$_4$-4-F	1.00
C$_6$H$_4$-4-Bu^t	0.21
C$_6$H$_4$-4-OMe	0.19
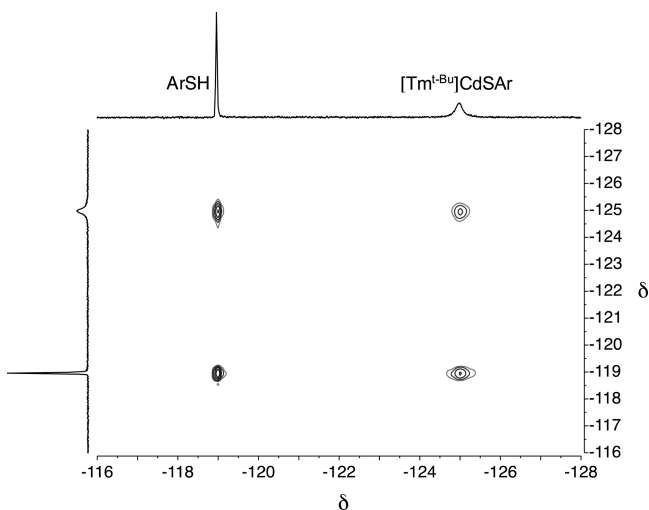
Figure 10. ^{19}F two-dimensional EXSY experiment demonstrating exchange of the SAr groups between [Tm$^{Bu^t}$]CdSAr and Ar′SH (Ar′ = C$_6$H$_4$-4-F).

spectra are reported in parts per million relative to SiMe$_4$ (δ 0) and were referenced internally with respect to the solvent (δ 128.06 for C$_6$D$_6$ and δ 53.84 for CD$_2$Cl$_2$).[63] ^{19}F NMR spectra are reported in parts per million relative to CFCl$_3$ (δ 0) and were referenced internally with respect to C$_6$F$_6$ (δ −164.9).[64] Coupling constants are given in hertz. Infrared (IR) spectra were recorded on a PerkinElmer Spectrum Two spectrometer, and the data are reported in reciprocal centimeters. Mass spectra were recorded on a JEOL JMS-HX110HF tandem mass spectrometer using fast atom bombardment (FAB). 4-Fluorothiophenol (Aldrich), 4-*tert*-butylbenzenethiol (Acros), 4-methoxythiophenol (Aldrich), 3-methoxythiophenol (Aldrich), and pyridine-2-thione (Aldrich) were obtained commercially and used without further purification. [Tm$^{Bu^t}$]CdMe[24,27] and pyridine-2-selone[65] were prepared by literature procedures.

X-ray Structure Determinations. X-ray diffraction data were collected on a Bruker Apex II diffractometer, and crystal data, data collection, and refinement parameters are summarized in the Supporting Information. The structures were determined by using direct methods and standard difference map techniques and refined by full-matrix least-squares procedures on F^2 with SHELXTL (version 2014/7).[66]

Synthesis of [Tm$^{Bu^t}$]CdSC$_6$H$_4$-4-F. A solution of [Tm$^{Bu^t}$]CdMe (218 mg, 0.361 mmol) in C$_6$H$_6$ (∼9 mL) was treated with 4-fluorothiophenol (40.0 μL, 0.375 mmol), resulting in immediate effervescence. The mixture was stirred at room temperature, and the volatile components were removed *in vacuo* after a period of 40 min.

The resulting powder was washed with Et$_2$O (∼2 mL) to give [Tm$^{Bu^t}$]-CdSC$_6$H$_4$-4-F as a white solid (130 mg, 50%). Crystals of [Tm$^{Bu^t}$]-CdSC$_6$H$_4$-4-F suitable for X-ray diffraction were obtained via slow diffusion of pentane into a solution in benzene. Anal. Calcd for [Tm$^{Bu^t}$]CdSC$_6$H$_4$-4-F: C, 45.2%; H, 5.3%; N, 11.7%. Found: C, 45.2%; H, 4.9%; N, 11.6%. ^{1}H NMR (C$_6$D$_6$): δ 1.41 (s, 27H, HB{C$_2$N$_2$H$_2$[C-(C$\underline{H}_3$)$_3$CS}$_3$), 6.37 (d, $^3J_{H-H}$ = 2, 3H, HB{C$_2$N$_2$$\underline{H}_2$[C(CH$_3$)$_3$CS}$_3$), 6.62 (d, $^3J_{H-H}$ = 2, 3H, HB{C$_2$N$_2$H$_2$[C(CH$_3$)$_3$CS}$_3$), 6.77 (m, 2H, CdSC$_6$$\underline{H}_4$-4-F), 7.86 (m, 2H, CdSC$_6$$\underline{H}_4$-4-F). ^{13}C{^{1}H} NMR (C$_6$D$_6$): δ 28.7 (9C, HB{C$_2$N$_2$H$_2$[C(C$\underline{H}_3$)$_3$CS}$_3$), 59.4 (3C, HB{C$_2$N$_2$H$_2$[$\underline{C}$-(CH$_3$)$_3$CS}$_3$), 114.7 (d, $^2J_{C-F}$ = 21, 2C, CdSC$_6$$\underline{H}_4$-4-F), 117.0 (3C, HB{$\underline{C}_2N_2H_2$[C(CH$_3$)$_3$CS}$_3$), 122.9 (3C, HB{$\underline{C}_2N_2H_2$[C(CH$_3$)$_3$-CS}$_3$), 135.7 (d, $^3J_{C-F}$ = 7, 2C, CdSC$_6$$\underline{H}_4$-4-F), 139.9 (d, $^4J_{C-F}$ = 3, 1C, CdSC$_6$$\underline{H}_4$-4-F), 157.2 (3C, HB{C$_2N_2H_2$[C(CH$_3$)$_3$$\underline{C}$S}$_3$), 160.6 (d, $^1J_{C-F}$ = 240, 1C, CdS$\underline{C}_6$H$_4$-4-F). ^{19}F NMR (C$_6$D$_6$): δ −125.1. IR data for [Tm$^{Bu^t}$]CdSC$_6$H$_6$-4-F (ATR, cm^{-1}): 3182 (w), 2977 (w), 2926 (w), 2404 (w), 2290 (w), 2227 (w), 2162 (w), 2051 (w), 1980 (w), 1719 (w), 1585 (w), 1566 (w), 1483 (s), 1416 (m), 1397 (m), 1357 (vs), 1304 (m), 1254 (w), 1221 (m), 1192 (vs), 1171 (s), 1129 (m), 1088 (s), 1070 (m), 1061 (m), 1033 (w), 1014 (w), 984 (w), 929 (w), 819 (s), 773 (w), 757 (m), 732 (s), 688 (s), 626 (vs), 589 (m), 553 (m), 544 (w), 497 (m), 480 (w), 455 (w). FAB-MS: m/z 591.2 [M − SC$_6$H$_4$-4-F]$^+$, M = [Tm$^{Bu^t}$]CdSC$_6$H$_4$-4-F.

Synthesis of [Tm$^{Bu^t}$]CdSC$_6$H$_4$-4-OMe. A solution of [Tm$^{Bu^t}$]CdMe (142 mg, 0.235 mmol) in C$_6$H$_6$ (∼5 mL) was treated with 4-methoxythiophenol (37.5 μL, 0.305 mmol), resulting in immediate effervescence. The mixture was stirred at room temperature for 45 min, after which period the volatile components were removed *in vacuo*. The resulting powder was washed with pentane (∼3 mL), yielding [Tm$^{Bu^t}$]CdSC$_6$H$_4$-4-OMe as a white solid (107 mg, 63%). Crystals of [Tm$^{Bu^t}$]CdSC$_6$H$_4$-4-OMe suitable for X-ray diffraction were obtained via slow diffusion of pentane into a solution in benzene. Anal. Calcd for [Tm$^{Bu^t}$]CdSC$_6$H$_4$-4-OMe·C$_6$H$_6$: C, 50.6%; H, 5.9%; N, 10.4%. Found: C, 51.0%; H, 5.7%; N, 10.0%. ^{1}H NMR (C$_6$D$_6$): δ 1.43 (s, 27H, HB{C$_2$N$_2$H$_2$[C(C$\underline{H}_3$)$_3$CS}$_3$), 3.34 (s, 3H, CdSC$_6$H$_4$-4-OC$\underline{H}_3$), 6.37 (d, $^3J_{H-H}$ = 2, 3H, HB{C$_2$N$_2$$\underline{H}_2$[C(CH$_3$)$_3$CS}$_3$), 6.63 (d, $^3J_{H-H}$ = 2, 3H, HB{C$_2$N$_2$$\underline{H}_2$[C(CH$_3$)$_3$CS}$_3$), 6.73 (d, $^3J_{H-H}$ = 8, 2H, CdSC$_6$$\underline{H}_4$-4-OMe), 7.94 (d, $^3J_{H-H}$ = 8, 2H, CdSC$_6$$\underline{H}_4$-4-OMe). ^{13}C{^{1}H} NMR (CD$_2$Cl$_2$): δ 29.1 (9C, HB{C$_2$N$_2$H$_2$[C(C$\underline{H}_3$)$_3$CS}$_3$), 55.6 [1C, CdS(C$_6$H$_4$-4-OC$\underline{H}_3$)], 59.8 (3C, HB{C$_2$N$_2$H$_2$[$\underline{C}$(CH$_3$)$_3$CS}$_3$), 113.9 [2C, CdS($\underline{C}_6$H$_4$-4-OMe)], 117.2 (3C, HB{$\underline{C}_2$N$_2$H$_2$[C(CH$_3$)$_3$CS}$_3$), 123.4 (3C, HB{$\underline{C}_2$N$_2$H$_2$[C(CH$_3$)$_3$CS}$_3$), 128.7 [1C, CdS($\underline{C}_6$H$_4$-4-OMe)], 134.6 [2C, CdS($\underline{C}_6$H$_4$-4-OMe)], 156.2 (3C, HB{C$_2$N$_2$H$_2$[C(CH$_3$)$_3$$\underline{C}$S}$_3$), 156.4 (1C, CdS$\underline{C}_6H_4$-4-OMe). IR data for [Tm$^{Bu^t}$]-CdSC$_6H_6$-4-OMe (ATR, cm^{-1}): 3174 (w), 3130 (w), 3097 (w), 2971 (w), 2833 (w), 2458 (w), 1590 (m), 1565 (m), 1486 (s), 1464 (w), 1416 (m), 1398 (m), 1356 (vs), 1301 (m), 1279 (w), 1263 (w), 1229 (s), 1192 (s), 1173 (w), 1132 (m), 1087 (w), 1071 (w), 1031 (m), 1018 (m), 927 (w), 822 (s), 773 (m), 756 (m), 744 (m), 730 (s), 684 (vs), 638 (m), 622 (m), 589 (m), 552 (m), 528 (m), 493 (m), 455 (m). FAB-MS: m/z 591.2 [M − SC$_6$H$_4$-4-OMe]$^+$, M = [Tm$^{Bu^t}$]CdSC$_6$H$_4$-4-OMe.

Synthesis of [Tm$^{Bu^t}$]CdSC$_6$H$_4$-3-OMe. A solution of [Tm$^{Bu^t}$]CdMe (106 mg, 0.175 mmol) in C$_6$H$_6$ (∼10 mL) was treated with 3-methoxythiophenol (30.0 μL, 0.242 mmol), resulting in immediate effervescence. The mixture was stirred at room temperature for 1 h, after which period the volatile components were removed *in vacuo*. The resulting

powder was washed with pentane (2 × 3 mL) and Et$_2$O (∼3 mL), yielding [Tm$^{Bu^t}$]CdSC$_6$H$_4$-3-OMe as a white solid (86 mg, 67%). Crystals of [Tm$^{Bu^t}$]CdSC$_6$H$_4$-3-OMe suitable for X-ray diffraction were obtained via slow diffusion of pentane into a solution in benzene. Anal. Calcd for [Tm$^{Bu^t}$]CdSC$_6$H$_4$-3-OMe·C$_6$H$_6$: C, 50.6%; H, 5.9%; N, 10.4%. Found: C, 51.3%; H, 5.6%; N, 9.9%. ^{1}H NMR (CD$_2$Cl$_2$): δ 1.71 (s, 27H, HB{C$_2$N$_2$H$_2$[C(C$\underline{H}_3$)$_3$]CS}$_3$), 3.71 (s, 3H, CdSC$_6$H$_4$-4-O$\underline{Me}$), 6.43 (d, $^3J_{H-H}$ = 8, 1H, CdSC$_6\underline{H}_4$-4-OMe), 6.84 (m, 1H, CdSC$_6\underline{H}_4$-4-OMe), 6.85 (d, $^3J_{H-H}$ = 2, 3H, HB{C$_2$N$_2\underline{H}_2$[C(CH$_3$)$_3$]CS}$_3$), 6.94 (m, 2H, CdSC$_6\underline{H}_4$-4-OMe), 7.03 (d, $^3J_{H-H}$ = 2, 3H, HB{C$_2$N$_2\underline{H}_2$-[C(CH$_3$)$_3$]CS}$_3$). ^{13}C{^{1}H} NMR (CD$_2$Cl$_2$): δ 29.1 (9C, HB-{C$_2$N$_2$H$_2$[C(C$\underline{H}_3$)$_3$]CS}$_3$), 55.4 (1C, CdSC$_6$H$_4$-3-O$\underline{C}$H$_3$), 59.8 (3C, HB{C$_2$N$_2$H$_2$[$\underline{C}$(CH$_3$)$_3$]CS}$_3$), 109.2 (1C, CdS$\underline{C}_6$H$_4$-3-OMe), 117.2 (3C, HB{$\underline{C}_2$N$_2$H$_2$[C(CH$_3$)$_3$]CS}$_3$), 118.4 (1C, CdS$\underline{C}_6$H$_4$-3-OMe), 123.5 (3C, HB{$\underline{C}_2$N$_2$H$_2$[C(CH$_3$)$_3$]CS}$_3$), 126.4 (1C, CdS$\underline{C}_6$H$_4$-3-OCH$_3$), 128.6 (1C, CdS$\underline{C}_6$H$_4$-3-OCH$_3$), 156.0 (3C, HB{C$_2$N$_2$H$_2$[C(CH$_3$)$_3$]$\underline{C}$S}$_3$), 159.5 (1C, CdS$\underline{C}_6$H$_4$-3-OMe) (*ipso* and *meta* C of C$_6$H$_4$-3-OMe not observed). IR data for [Tm$^{Bu^t}$]CdSC$_6$H$_6$-3-OMe (ATR, cm^{-1}): 3190 (w), 3148 (w), 2974 (w), 2404 (w), 1585 (m), 1566 (m), 1481 (m), 1467 (m), 1417 (m), 1397 (w), 1357 (vs), 1303 (m), 1274 (m), 1222 (m), 1191 (s), 1172 (s), 1131 (m), 1097 (m), 1070 (m), 1041 (m), 930 (w), 854 (m), 844 (m), 820 (m), 757 (m), 733 (s), 686 (vs), 588 (m), 552 (m), 494 (m). FAB-MS: *m/z* 591.2 [M − SC$_6$H$_4$-3-OMe]$^+$, M = [Tm$^{Bu^t}$]CdSC$_6$H$_4$-3-OMe.

Synthesis of [Tm$^{Bu^t}$]CdSC$_6$H$_4$-4-Bu^t. A solution of [Tm$^{Bu^t}$]CdMe (143 mg, 0.237 mmol) in C$_6$H$_6$ (∼5 mL) was treated with 4-*tert*-butylbenzenethiol (47.5 μL, 0.275 mmol), resulting in immediate effervescence. The mixture was stirred at room temperature for 45 min, after which period the volatile components were removed *in vacuo*. The resulting powder was washed with pentane (∼3 mL) to give [Tm$^{Bu^t}$]CdSC$_6$H$_4$-4-Bu^t as a white solid (117 mg, 66%). Crystals of [Tm$^{Bu^t}$]CdSC$_6$H$_4$-4-Bu^t suitable for X-ray diffraction were obtained via slow diffusion of pentane into a solution in benzene. Anal. Calcd for [Tm$^{Bu^t}$]CdSC$_6$H$_4$-4-Bu^t·0.7C$_6$H$_6$: C, 52.2%; H, 6.4%; N, 10.4%. Found: C, 51.8%; H, 6.2%; N, 9.5%. ^{1}H NMR (CD$_2$Cl$_2$): δ 1.24 [s, 9H, CdS(C$_6$H$_4$-4-$\underline{Bu}^t$)], 1.71 (s, 27H, HB{C$_2$N$_2$H$_2$[C(C$\underline{H}_3$)$_3$]CS}$_3$), 6.85 (d, $^3J_{H-H}$ = 2, 3H, HB{C$_2$N$_2\underline{H}_2$[C(CH$_3$)$_3$]CS}$_3$), 6.97 (d, $^3J_{H-H}$ = 8, 2H, CdSC$_6\underline{H}_4$-4-Bu^t), 7.03 (d, $^3J_{H-H}$ = 2, 3H, HB{C$_2$N$_2\underline{H}_2$[C(CH$_3$)$_3$]CS}$_3$), 7.25 (d, $^3J_{H-H}$ = 8, 2H, CdSC$_6\underline{H}_4$-4-Bu^t). ^{13}C{^{1}H} NMR (C$_6$D$_6$): δ 29.1 (9C, HB{C$_2$N$_2$H$_2$[C(C$\underline{H}_3$)$_3$]CS}$_3$), 31.6 {3C, CdS[C$_6$H$_4$-4-C(C$\underline{H}_3$)$_3$]}, 34.3 {1C, CdS[C$_6$H$_4$-4-$\underline{C}$(CH$_3$)$_3$]}, 59.8 (3C, HB{C$_2$N$_2$H$_2$[$\underline{C}$(CH$_3$)$_3$]CS}$_3$), 117.2 (3C, HB{$\underline{C}_2$N$_2$H$_2$[C(CH$_3$)$_3$]CS}$_3$), 123.4 (3C, HB{$\underline{C}_2$N$_2$H$_2$[C(CH$_3$)$_3$]CS}$_3$), 125.1 (2C, CdS$\underline{C}_6$H$_4$-4-Bu^t), 133.2 (2C, CdS$\underline{C}_6$H$_4$-4-Bu^t), 139.4 (1C, CdS$\underline{C}_6$H$_4$-4-Bu^t), 145.5 (1C, CdS$\underline{C}_6$H$_4$-4-Bu^t), 156.1 (3C, HB{C$_2$N$_2$H$_2$[C(CH$_3$)$_3$]$\underline{C}$S}$_3$).

Synthesis of [Tm$^{Bu^t}$]CdSPy. A solution of [Tm$^{Bu^t}$]CdMe (83.3 mg, 0.138 mmol) in C$_6$H$_6$ (∼5 mL) was treated with pyridine-2-thione (20.2 mg, 0.182 mmol), and the mixture was stirred at room temperature for 4.5 h. After this period, the volatile components were removed *in vacuo*, yielding [Tm$^{Bu^t}$]CdSPy as a yellow powder, and crystals suitable for X-ray diffraction were obtained by diffusion of pentane into a solution in benzene (60 mg, 62%). Anal. Calcd for [Tm$^{Bu^t}$]CdSPy: C, 44.6%; H, 5.5%; N, 14.0%. Found: C, 44.9%; H, 5.5%; N, 13.7%. ^{1}H NMR (CD$_2$Cl$_2$): δ 1.74 (s, 27H, HB{C$_2$N$_2$H$_2$[C-(C$\underline{H}_3$)$_3$]CS}$_3$), 6.67 (m, 1H, CdSC$_5\underline{H}_4$N), 6.86 (d, $^3J_{H-H}$ = 2, 3H, HB{C$_2$N$_2\underline{H}_2$[C(CH$_3$)$_3$]CS}$_3$), 7.04 (d, $^3J_{H-H}$ = 2, 3H, HB{C$_2$N$_2\underline{H}_2$[C-(CH$_3$)$_3$]CS}$_3$), 7.23 (m, 1H, CdSC$_5\underline{H}_4$N), 7.28 (m, 1H, CdSC$_5\underline{H}_4$N), 7.76 (m, 1H, CdSC$_5\underline{H}_4$N). ^{13}C{^{1}H} NMR (CD$_2$Cl$_2$): 29.2 (9C, HB{C$_2$N$_2$H$_2$[C(C$\underline{H}_3$)$_3$]CS}$_3$), 59.6 (3C, HB{C$_2$N$_2$H$_2$[$\underline{C}$(CH$_3$)$_3$]-CS}$_3$), 116.0 (1C, CdSC$_5$H$_4$N), 117.0 (3C, HB{$\underline{C}_2$N$_2$H$_2$[C(CH$_3$)$_3$]-CS}$_3$), 123.2 (3C, HB{$\underline{C}_2$N$_2$H$_2$[C(CH$_3$)$_3$]CS}$_3$), 125.1 (1C, CdSC$_5$H$_4$N), 136.1 (1C, CdS$\underline{C}_5$H$_4$N), 147.3 (1C, CdS$\underline{C}_5$H$_4$N), 156.9 (3C, HB{C$_2$N$_2$H$_2$[C(CH$_3$)$_3$]$\underline{C}$S}$_3$), 171.9 (1C, CdS$\underline{C}_5$H$_4$N). IR data for [Tm$^{Bu^t}$]CdSPy (ATR, cm^{-1}): 3173 (w), 3140 (w), 2977 (w), 2923 (w), 2404 (w), 2228 (w), 1686 (w), 1567 (m), 1545 (m), 1479 (w), 1445 (m), 1411 (m), 1396 (m), 1355 (vs), 1303 (m), 1265 (w), 1227 (m), 1191 (s), 1172 (s), 1130 (s), 1071 (m), 1044 (w), 1029 (w), 986 (w), 928 (w), 862 (w), 820 (m), 774 (w), 758 (m), 749 (m), 731 (vs),

688 (s), 627 (w), 589 (m), 553 (m), 545 (m), 494 (m), 487 (m). FAB-MS: *m/z* 589.1 [M − SPy]$^+$, M = [Tm$^{Bu^t}$]CdSPy.

Synthesis of [Tm$^{Bu^t}$]CdSePy. A solution of [Tm$^{Bu^t}$]CdMe (86.5 mg, 0.143 mmol) in C$_6$H$_6$ (∼5 mL) was treated with pyridine-2-selone (30.3 mg, 0.192 mmol), and the mixture was stirred at room temperature for 4.5 h. After this period, the volatile components were removed *in vacuo*, yielding [Tm$^{Bu^t}$]CdSePy as a dark yellow-orange powder, and crystals suitable for X-ray diffraction were obtained by diffusion of pentane into a solution in benzene (63 mg, 59%). Anal. Calcd for [Tm$^{Bu^t}$]CdSePy: C, 41.8%; H, 5.1%; N, 13.1%. Found: C, 41.0%; H, 4.8%; N, 12.7%. ^{1}H NMR (CD$_2$Cl$_2$): δ 1.74 (s, 27H, HB{C$_2$N$_2$H$_2$[C-(C$\underline{H}_3$)$_3$]CS}$_3$), 6.78 (m, 1H, CdSeC$_5\underline{H}_4$N), 6.86 (d, $^3J_{H-H}$ = 2, 3H, HB{C$_2$N$_2\underline{H}_2$[C(CH$_3$)$_3$]CS}$_3$), 7.04 (d, $^3J_{H-H}$ = 2, 3H, HB{C$_2$N$_2\underline{H}_2$[C-(CH$_3$)$_3$]CS}$_3$), 7.17 (m, 1H, CdSeC$_5\underline{H}_4$N), 7.48 (m, 1H, CdSeC$_5\underline{H}_4$N), 7.82 (m, 1H, CdSeC$_5\underline{H}_4$N). ^{13}C{^{1}H} NMR (CD$_2$Cl$_2$): δ 29.2 (9C, HB{C$_2$N$_2$H$_2$[C(C$\underline{H}_3$)$_3$]CS}$_3$), 59.6 (3C, HB{C$_2$N$_2$H$_2$[$\underline{C}$(CH$_3$)$_3$]CS}$_3$), 117.0 (3C, HB{$\underline{C}_2$N$_2$H$_2$[C(CH$_3$)$_3$]CS}$_3$), 117.4 (1C, CdSe$\underline{C}_5$H$_4$N), 123.2 (3C, HB{$\underline{C}_2$N$_2$H$_2$[C(CH$_3$)$_3$]CS}$_3$), 128.8 (1C, CdSe$\underline{C}_5$H$_4$N), 135.4 (1C, CdSe$\underline{C}_5$H$_4$N), 148.6 (1C, CdSe$\underline{C}_5$H$_4$N), 156.9 (3C, HB{C$_2$N$_2$H$_2$[C(CH$_3$)$_3$]$\underline{C}$S}$_3$), 163.7 (1C, CdSe$\underline{C}_5$H$_4$N). IR data for [Tm$^{Bu^t}$]CdSePy (ATR, cm^{-1}): 3185 (w), 2975 (w), 2924 (w), 2404 (w), 2227 (w), 1686 (w), 1574 (w), 1547 (w), 1480 (w), 1445 (w), 1409 (m), 1396 (w), 1356 (vs), 1303 (m), 1267 (w), 1227 (m), 1191 (s), 1172 (s), 1129 (m), 1113 (s), 1081 (w), 1070 (w), 1045 (w), 1030 (w), 983 (w), 929 (w), 864 (w), 821 (m), 774 (w), 757 (m), 750 (m), 731 (vs), 699 (m), 689 (s), 621 (w), 589 (m), 553 (m), 494 (m), 471 (m), 454 (w). FAB-MS: *m/z* 591.1 [M − SePy]$^+$, M = [Tm$^{Bu^t}$]CdSePy.

Thiolate Exchange between [Tm$^{Bu^t}$]CdSAr and Ar′SH. (a) A solution of [Tm$^{Bu^t}$]CdSC$_6$H$_4$-4-F in C$_6$D$_6$ (0.7 mL) was treated with ArSH (Ar = C$_6$H$_4$-4-Bu^t or C$_6$H$_4$-4-OMe, 1 equiv), and the sample was monitored by ^{1}H NMR spectroscopy, thereby demonstrating the formation of an equilibrium mixture (Table 5). As previously noted,[56c] hydrogen bonding is not considered to perturb the equilibrium constant significantly. (b) A solution of [Tm$^{Bu^t}$]CdSC$_6$H$_4$-4-F in C$_6$D$_6$ (0.7 mL) was treated with 4-fluorothiophenol, and exchange at room temperature was demonstrated by a ^{19}F two-dimensional EXSY experiment.

■ ASSOCIATED CONTENT

Ⓢ Supporting Information

The Supporting Information is available free of charge on the ACS Publications website at DOI: 10.1021/acs.inorgchem.7b00296.

　　Tables of crystallographic information (PDF)
　　Crystallographic data (ZIP)

■ AUTHOR INFORMATION

Corresponding Author
*E-mail: jso2115@columbia.edu. (J.S.O.)
*E-mail: parkin@columbia.edu. (G.P.).

ORCID ⦿
Jonathan S. Owen: 0000-0001-5502-3267
Gerard Parkin: 0000-0003-1925-0547

Notes
The authors declare no competing financial interest.

■ REFERENCES

(1) (a) Dance, I. G. The structural chemistry of metal thiolate complexes. *Polyhedron* **1986**, *5*, 1037−1104. (b) Blower, P. J.; Dilworth, J. R. Thiolato-complexes of the transition metals. *Coord. Chem. Rev.* **1987**, *76*, 121−185. (c) Gimeno, M. C. Thiolates, Selenolates, and Tellurolates. *Handbook of Chalcogen Chemistry*; Royal Society of Chemistry: London, 2007; Chapter 2.1, pp 33−80.

(2) (a) Holm, R. H.; Ciurli, S.; Weigel, J. A. Subsite-specific structures and reactions in native and synthetic [4Fe-4S] cubane-type clusters. *Prog. Inorg. Chem.* **1990**, *38*, 1−74. (b) Krebs, B.; Henkel, G. Transition-metal thiolates: from molecular fragments of sulfidic solids to models for active centers in biomolecules. *Angew. Chem., Int. Ed. Engl.* **1991**, *30*, 769−788. (c) Coucouvanis, D. Use of preassembled Fe/S and Fe/Mo/S clusters in the stepwise synthesis of potential analoues ofr the Fe/Mo/S site in nitrogenase. *Acc. Chem. Res.* **1991**, *24*, 1−8. (d) Mohamed, A. A.; Abdou, H. E.; Chen, J.; Bruce, A. E.; Bruce, M. R. M. Perspectives in Inorganic and Bioinorganic gold sulfur chemistry. *Comments Inorg. Chem.* **2002**, *23*, 321−334. (e) Solomon, E. I.; Gorelsky, S. I.; Dey, A. Metal-thiolate bonds in bioinorganic chemistry. *J. Comput. Chem.* **2006**, *27*, 1415−1428. (f) Ohki, Y.; Tatsumi, K. Thiolate-bridged iron-nickel models for the active site of [NiFe] hydrogenase. *Eur. J. Inorg. Chem.* **2011**, *2011*, 973−985. (g) Stiefel, E. I. Transition metal sulfur chemistry: Biological and industrial significance and key trends. *ACS Symp. Ser.* **1996**, *653*, 2−38. (h) García-Vázquez, J. A.; Romero, J.; Sousa, A. Electrochemical synthesis of metallic complexes of bidentate thiolates containing nitrogen as an additional donor atom. *Coord. Chem. Rev.* **1999**, *193−195*, 691−745.

(3) (a) Owen, J. S.; Park, J.; Trudeau, P.-E.; Alivisatos, A. P. Reaction chemistry and ligand exchange at cadmium-selenide nanocrystal surfaces. *J. Am. Chem. Soc.* **2008**, *130*, 12279−12281. (b) Gaponik, N.; Talapin, D. V.; Rogach, A. L.; Hoppe, K.; Shevchenko, E. V.; Kornowski, A.; Eychmuller, A.; Weller, H. Thiol-Capping of CdTe Nanocrystals: An alternative to Organometallic Synthetic Routes. *J. Phys. Chem. B* **2002**, *106*, 7177−7185. (c) Jin, R. Quantum sized, thiolate-protected gold nanoclusters. *Nanoscale* **2010**, *2*, 343−362. (d) Gao, M.; Lesser, C.; Kirstein, S.; Möhwald, H.; Rogach, A. L.; Weller, H. Electroluminescence of different colors from polycation/CdTe nanocrystal self-assembled films. *J. Appl. Phys.* **2000**, *87*, 2297−2302.

(4) (a) Holm, R. H.; Kennepohl, P.; Solomon, E. I. Structural and functional aspects of metal sites in biology. *Chem. Rev.* **1996**, *96*, 2239−2314. (b) Lipscomb, W. N.; Sträter, N. Recent advances in zinc enzymology. *Chem. Rev.* **1996**, *96*, 2375−2433.

(5) (a) Maret, W. Zinc biochemistry: From a single zinc enzyme to a key element of life. *Adv. Nutr.* **2013**, *4*, 82−91. (b) Maret, W. New perspectives of zinc coordination environments in proteins. *J. Inorg. Biochem.* **2012**, *111*, 110−116. (c) Maret, W. Zinc and sulfur: A critical biological partnership. *Biochemistry* **2004**, *43*, 3301−3309. (d) Iuchi, S. Three classes of C_2H_2 zinc finger proteins. *Cell. Mol. Life Sci.* **2001**, *58*, 625−635. (e) Laity, J. H.; Lee, B. M.; Wright, P. E. Zinc finger proteins: new insights into structural and functional diversity. *Curr. Opin. Struct. Biol.* **2001**, *11*, 39−46. (f) Karlin, S.; Zhu, Z.-Y. Classification of mononuclear zinc metal sites in protein structures. *Proc. Natl. Acad. Sci. U. S. A.* **1997**, *94*, 14231−14236.

(6) (a) Simonson, T.; Calimet, N. $Cys_xHis_y−Zn^{2+}$ Interactions: Thiol vs. thiolate coordination. *Proteins: Struct., Funct., Genet.* **2002**, *49*, 37−48. (b) Dudev, T.; Lim, C. Factors governing the protonation state of cysteines in proteins: An ab initio/CDM study. *J. Am. Chem. Soc.* **2002**, *124*, 6759−6766.

(7) (a) Parkin, G. Synthetic analogues relevant to the structure and function of zinc enzymes. *Chem. Rev.* **2004**, *104*, 699−767. (b) Parkin, G. Synthetic analogues of zinc enzymes. In *Metal Ions in Biological Systems*; Sigel, A., Sigel, H., Eds.; Marcel Dekker: New York, 2001; Vol. 38, Chapter 14, pp 411−460.

(8) The cadmium enzyme was discovered in marine diatoms. See: (a) Lane, T. W.; Saito, M. A.; George, G. N.; Pickering, I. J.; Prince, R. C.; Morel, F. M. M. A cadmium enzyme from a marine diatom. *Nature* **2005**, *435*, 42. (b) Lane, T. W.; Morel, F. M. M. A biological function for cadmium in marine diatoms. *Proc. Natl. Acad. Sci. U. S. A.* **2000**, *97*, 4627−4631.

(9) (a) Maret, W.; Moulis, J. M. The bioinorganic chemistry of cadmium in the context of its toxicity. *Met. Ions Life Sci.* **2013**, *11*, 1−29. (b) Thevenod, F.; Lee, W. K. Toxicology of cadmium and its damage to mammalian organs. *Met. Ions Life Sci.* **2013**, *11*, 415−490. (c) Nordberg, G. F. Historical perspectives on cadmium toxicology. *Toxicol. Appl. Pharmacol.* **2009**, *238*, 192−200. (d) Remelli, M.; Nurchi, V. M.; Lachowicz, J. I.; Medici, S.; Zoroddu, M. A.; Peana, M. Competition between Cd(II) and other divalent transition metal ions during complex formation with amino acids, peptides, and chelating agents. *Coord. Chem. Rev.* **2016**, *327−328*, 55−69.

(10) Friedman, R. Structural and computational insights into the versatility of cadmium binding to proteins. *Dalton Trans.* **2014**, *43*, 2878−2887.

(11) Klaassen, C. D.; Liu, J.; Diwan, B. A. Metallothionein protection of cadmium toxicity. *Toxicol. Appl. Pharmacol.* **2009**, *238*, 215−220.

(12) (a) Isani, G.; Carpenè, E. Metallothioneins, unconventional proteins from unconventional animals: A long journey from nematodes to mammals. *Biomolecules* **2014**, *4*, 435−457. (b) Stillman, M. J. Metallothioneins. *Coord. Chem. Rev.* **1995**, *144*, 461−511.

(13) (a) Zillner, E.; Fengler, S.; Niyamakom, P.; Rauscher, F.; Köhler, K.; Dittrich, T. Role of ligand exchange at CdSe quantum dot layers for charge separation. *J. Phys. Chem. C* **2012**, *116*, 16747−16754. (b) Liu, F.; Zhu, J.; Wei, J.; Li, Y.; Hu, L.; Huang, Y.; Takuya, O.; Shen, Q.; Toyoda, T.; Zhang, B.; Yao, J.; Dai, S. Ex situ CdSe quantum dot-sensitized solar cells employing inorganic ligand exchange to boost efficiency. *J. Phys. Chem. C* **2014**, *118*, 214−222. (c) Rosenthal, S. J.; McBride, J.; Pennycook, S. J.; Feldman, L. C. Synthesis, surface studies, composition and structural characterization of CdSe, core/shell and biologically active nanocrystals. *Surf. Sci. Rep.* **2007**, *62*, 111−157. (d) Talapin, D. V.; Lee, J.-S.; Kovalenko, M. V.; Shevchenko, E. V. Prospects of colloidal nanocrystals for electronic and optoelectronic applications. *Chem. Rev.* **2010**, *110*, 389−458. (e) Guyot-Sionnest, P.; Wehrenberg, B.; Yu, D. Intraband relaxation in CdSe nanocrystals and the strong influence of the surface ligands. *J. Chem. Phys.* **2005**, *123*, 074709. (f) Pandey, A.; Guyot-Sionnest, P. Slow electron cooling in colloidal quantum dots. *Science* **2008**, *322*, 929−932. (g) Tang, J.; Kemp, K. W.; Hoogland, S.; Jeong, K. S.; Liu, H.; Levina, L.; Furukawa, M.; Wang, X.; Debnath, R.; Cha, D.; Chou, K. W.; Fischer, A.; Amassian, A.; Asbury, J. B.; Sargent, E. H. Colloidal-quantum-dot photovoltaics using atomic-ligand passivation. *Nat. Mater.* **2011**, *10*, 765−771.

(14) (a) Spicer, M. D.; Reglinski, J. Soft scorpionate ligands based on imidazole-2-thione donors. *Eur. J. Inorg. Chem.* **2009**, *2009*, 1553−1574. (b) Smith, J. M. Strongly donating scorpionate ligands. *Comments Inorg. Chem.* **2008**, *29*, 189−233. (c) Soares, L. F.; Silva, R. M. Hydrotris-(methimazolyl)borate. *Inorg. Synth.* **2002**, *33*, 199−202. (d) Rabinovich, D. Poly(mercaptoimidazolyl)borate complexes of cadmium and mercury. *Struct. Bonding (Berlin)* **2006**, *120*, 143−162.

(15) (a) Parkin, G. The bioinorganic chemistry of zinc: synthetic analogues of zinc enzymes that feature tripodal ligands. *Chem. Commun.* **2000**, 1971−1985. (b) Parkin, G. Applications of tripodal [S_3] and [Se_3] L_2X donor ligands to zinc, cadmium and mercury chemistry: organometallic and bioinorganic perspectives. *New J. Chem.* **2007**, *31*, 1996−2014.

(16) (a) Vahrenkamp, H. Transitions, transition states, transition state analogues: Zinc pyrazolylborate chemistry related to zinc enzymes. *Acc. Chem. Res.* **1999**, *32*, 589−596. (b) Vahrenkamp, H. *Bioinorganic Chemistry: Transition Metals in Biology and their Coordination Chemistry*; Wiley-VCH: Weinheim, Germany, 1997; pp 540−551. (c) Vahrenkamp, H. Why does nature use zinc - a personal view. *Dalton Trans.* **2007**, 4751−4759.

(17) Kreider-Mueller, A.; Rong, Y.; Owen, J. S.; Parkin, G. Molecular structures of tris(2-mercapto-1-tert-butylimidazolyl)hydroborato and tris(2-mercapto-1-adamantylimidazolyl)hydroborato sodium complexes: analysis of [Tm^R] ligand coordination modes and conformations. *Dalton Trans.* **2014**, *43*, 10852−10865.

(18) Rajesekharan-Nair, R.; Lutta, S. T.; Kennedy, A. R.; Reglinski, J.; Spicer, M. D. Soft scorpionate coordination at alkali metals. *Acta Crystallogr., Sect. C: Struct. Chem.* **2014**, *70*, 421−427.

(19) (a) Green, M. L. H. A new approach to the formal classification of covalent compounds of the elements. *J. Organomet. Chem.* **1995**, *500*, 127−148. (b) Parkin, G. Classification of organotransition metal compounds. In *Comprehensive Organometallic Chemistry III*; Crabtree, R. H., Mingos, D. M. P., Eds.; Elsevier: Oxford, U.K., 2006; Vol. *1*, Chapter 1.01. (c) Green, J. C.; Green, M. L. H.; Parkin, G. The occurrence and representation of three-centre two-electron bonds in covalent inorganic compounds. *Chem. Commun.* **2012**, *48*, 11481−11503. (d) Green, M. L. H.; Parkin, G. Application of the Covalent Bond Classification method for the teaching of inorganic chemistry. *J. Chem. Educ.* **2014**, *91*, 807−816.

(20) (a) Bridgewater, B. M.; Fillebeen, T.; Friesner, R. A.; Parkin, G. A zinc thiolate species which mimics aspects of the chemistry of the Ada repair protein and matrix metalloproteinases: The synthesis, structure and reactivity of the tris(2-mercapto-1-phenylimidazolyl)hydroborato complex [Tm^{Ph}]ZnSPh. *J. Chem. Soc., Dalton Trans.* **2000**, 4494−4496. (b) Melnick, J. G.; Zhu, G.; Buccella, D.; Parkin, G. Thiolate exchange in [Tm^R]ZnSR′ complexes and relevance to the mechanisms of thiolate alkylation reactions involving zinc enzymes and proteins. *J. Inorg. Biochem.* **2006**, *100*, 1147−1154.

(21) Morlok, M. M.; Janak, K. E.; Zhu, G.; Quarless, D. A.; Parkin, G. Intramolecular N-H···S hydrogen bonding in the zinc thiolate complex [Tm^{Ph}]ZnSCH$_2$C(O)NHPh: A mechanistic investigation of thiolate alkylation as probed by kinetics studies and by kinetic isotope effects. *J. Am. Chem. Soc.* **2005**, *127*, 14039−14050.

(22) Bridgewater, B. M.; Parkin, G. A zinc hydroxide complex of relevance to 5-aminolevulinate dehydratase: The synthesis, structure and reactivity of the tris(2-mercapto-1-phenylimidazolyl)hydroborato Complex [Tm^{Ph}]ZnOH. *Inorg. Chem. Commun.* **2001**, *4*, 126−129.

(23) Bridgewater, B. M.; Parkin, G. Lead poisoning and the inactivation of 5-aminolevulinate dehydratase as modeled by the tris(2-mercapto-1-phenylimidazolyl)hydroborato lead complex, {[Tm^{Ph}]Pb}[ClO$_4$]. *J. Am. Chem. Soc.* **2000**, *122*, 7140−7141.

(24) Melnick, J. G.; Parkin, G. Methyl and arylchalcogenolate complexes of cadmium in a sulfur rich coordination environment: Syntheses and structural characterization of the tris(2-mercapto-1-tert-butylimidazolyl)hydroborato cadmium complexes [Tm$^{Bu^t}$]CdMe, and [Tm$^{Bu^t}$]CdEAr (E = O, S, Se, Te) and analysis of the bonding in chalcogenolate compounds. *Dalton Trans.* **2006**, 4207−4210.

(25) (a) Palmer, J. H.; Parkin, G. Synthesis and structural characterization of tris(2-mercapto-1-methylbenzimidazolyl) hydroborato cadmium halide complexes,{[Tm^{MeBenz}]Cd(μ-Cl)}$_2$ and [Tm^{MeBenz}]CdI: A rare example of cadmium in a trigonal bipyramidal sulfur-rich coordination environment. *Dalton Trans.* **2014**, *43*, 13874−13882. (b) Palmer, J. H.; Parkin, G. Influence of benzannulation on metal coordination geometries: Synthesis and structural character-ization of tris(2-mercapto-1- methylbenzimidazolyl)hydroborato cad-mium bromide, {[Tm^{MeBenz}]Cd(μ-Br)}$_2$. *J. Mol. Struct.* **2015**, *1081*, 530−535.

(26) Kreider-Mueller, A.; Quinlivan, P. J.; Owen, J. S.; Parkin, G. Synthesis and structures of cadmium carboxylate and thiocarboxylate compounds with a sulfur-rich coordination environment: Carboxylate exchange kinetics involving tris(2-mercapto-1-t-butylimidazolyl)-hydroborato cadmium complexes, [Tm$^{Bu^t}$]Cd(O$_2$CR). *Inorg. Chem.* **2015**, *54*, 3835−3850.

(27) Kreider-Mueller, A.; Quinlivan, P. J.; Rong, Y.; Owen, J. S.; Parkin, G. Exchange of alkyl and tris(2-mercapto-1-t-butylimidazolyl)-hydroborato ligands between zinc, cadmium and mercury. *J. Organomet. Chem.* **2015**, *792*, 177−183.

(28) (a) Bakbak, S.; Incarvito, C. D.; Rheingold, A. L.; Rabinovich, D. Synthesis and characterization of novel mononuclear cadmium thiolate complexes in a sulfur-rich environment. *Inorg. Chem.* **2002**, *41*, 998−1001. (b) Bakbak, S.; Bhatia, V. K.; Incarvito, C. D.; Rheingold, A. L.; Rabinovich, D. Synthesis and characterization of two new bulky tris(mercaptoimidazolyl)borate ligands and their zinc and cadmium complexes. *Polyhedron* **2001**, *20*, 3343−3348. (c) White, J. L.; Tanski, J. M.; Rabinovich, D. Bulky tris(mercaptoimidazolyl)borates: Synthesis and molecular structures of the group 12 metal complexes [Tm^{t-Bu}]MBr (M = Zn, Cd, Hg). *J. Chem. Soc., Dalton Trans.* **2002**, 2987−2991.

(29) (a) Cassidy, I.; Garner, M.; Kennedy, A. R.; Potts, G. B. S.; Reglinski, J.; Slavin, P. A.; Spicer, M. D. The preparation and structures of group 12 (Zn, Cd, Hg) complexes of the soft tripodal ligand hydrotris(methimazolyl)borate (Tm). *Eur. J. Inorg. Chem.* **2002**, *2002*, 1235−1239. (b) Bailey, P. J.; Dawson, A.; McCormack, C.; Moggach, S. A.; Oswald, I. D. H.; Parsons, S.; Rankin, D. W. H.; Turner, A. Barriers to racemization in *C*$_3$-symmetric complexes containing the hydrotris(2-mercapto-1-ethylimidazolyl)borate (Tm^{Et}) ligand. *Inorg. Chem.* **2005**, *44*, 8884−8898.

(30) (a) Melnick, J. G.; Parkin, G. Cleaving mercury-alkyl bonds: A functional model for mercury detoxification by MerB. *Science* **2007**, *317*, 225−227. (b) Melnick, J. G.; Yurkerwich, K.; Parkin, G. On the chalcogenophilicity of mercury: Evidence for a strong Hg-Se bond in [Tm^{Bu}]HgSePh and its relevance to the toxicity of mercury. *J. Am. Chem. Soc.* **2010**, *132*, 647−655.

(31) Cetin, A.; Ziegler, C. J. Coordinative flexibility in hydrotris-(methimazolyl)borate divalent metal compounds. *Dalton Trans.* **2006**, 1006−1008.

(32) Viktora, M. A.; He, X.; Hsieh, J.; Mihalcik, D. J.; Rabinovich, D. cited in ref 14d.

(33) $\tau_4 = [360 − (\alpha + \beta)]/141$, where α and β are the two largest angles. $\tau_\delta = \tau_4(\beta/\alpha)$, where $\alpha > \beta$. See: (a) Yang, L.; Powell, D. R.; Houser, R. P. Structural variation in copper(I) complexes with pyridylmethylamide ligands: Structural analysis with a new four-coordinate geometry index, τ. *Dalton Trans.* **2007**, 955−964. (b) Reineke, M. H.; Sampson, M. D.; Rheingold, A. L.; Kubiak, C. P. Synthesis and structural studies of nickel(0) tetracarbene complexes with the introduction of a new four-coordinate geometric index, τ_δ. *Inorg. Chem.* **2015**, *54*, 3211−3217.

(34) Haaland, A. Covalent versus dative bonds to main group metals, a useful distinction. *Angew. Chem., Int. Ed. Engl.* **1989**, *28*, 992−1007.

(35) Searches of the Cambridge Structural Database were performed with version 5.37. See: Groom, C. R.; Bruno, I. J.; Lightfoot, M. P.; Ward, S. C. The Cambridge Structural Database. *Acta Crystallogr., Sect. B: Struct. Sci., Cryst. Eng. Mater.* **2016**, *72*, 171−179.

(36) (a) Brookhart, M.; Green, M. L. H.; Parkin, G. Agostic interactions in transition metal compounds. *Proc. Natl. Acad. Sci. U. S. A.* **2007**, *104*, 6908−6914. (b) Brookhart, M.; Green, M. L. H.; Wong, L. L. Carbon-hydrogen-transition-metal bonds. *Prog. Inorg. Chem.* **1988**, *36*, 1−124. (c) Brookhart, M.; Green, M. L. H. Carbon-hydrogen-transition metal Bonds. *J. Organomet. Chem.* **1983**, *250*, 395−408.

(37) r_{cov}(Cd) = 1.44 Å, and r_{cov}(H) = 0.31 Å. See: Cordero, B.; Gómez, V.; Platero-Prats, A. E.; Revés, M.; Echeverría, J.; Cremades, E.; Barragán, F.; Alvarez, S. Covalent radii revisited. *Dalton Trans.* **2008**, 2832−2838.

(38) Pyridine-2-thiolate is also known as pyridine-2-thionate. See ref 40.

(39) Pyridine-2-thione exists in equilibrium with the pyridine-2-thiol tautomer (also known as 2-mercaptopyridine). See: Moran, D.; Sukcharoenphon, K.; Puchta, R.; Schaefer, H. F.; Schleyer, P. V.; Hoff, C. D. 2-pyridinethiol/2-pyridinethione tautomeric equilibrium. A comparative experimental and computational study. *J. Org. Chem.* **2002**, *67*, 9061−9069.

(40) (a) Raper, E. S. Complexes of heterocyclic thionates.1. Complexes of monodentate and chelating ligands. *Coord. Chem. Rev.* **1996**, *153*, 199−255. (b) Raper, E. S. Complexes of heterocyclic thionates.2. complexes of bridging ligands. *Coord. Chem. Rev.* **1997**, *165*, 475−567. (c) Raper, E. S. Complexes of heterocyclic thione donors. *Coord. Chem. Rev.* **1985**, *61*, 115−184. (d) Akrivos, P. D. Recent studies in the coordination chemistry of heterocyclic thiones and thionates. *Coord. Chem. Rev.* **2001**, *213*, 181−210.

(41) Hursthouse, M. B.; Khan, O. F. Z.; Mazid, M.; Motevalli, M.; O'Brien, P. The X-ray crystal structures of the cadmium complexes of pyridine-1-thiol and mercaptobenzothiazole, [Cd(C$_5$H$_4$NS)$_2$]$_n$ and [Cd(C$_7$H$_4$N$_2$S$_2$)$_2$]$_n$: Two unusual volatile polymeric complexes. *Polyhedron* **1990**, *9*, 541−544.

(42) In addition to pyridinethiolate complexes, pyridinethione adducts are also known. For example, see: (a) Wang, X.-J.; Ni, Q.-L.; Bi, X.-S.; Jian, H.-X. Dichlorobis(pyridinium-2-thiolato)cadmium(II). *Acta Crys-*

tallogr., Sect. E: Struct. Rep. Online 2004, 60, m1859−m1860. (b) Wen, Y.-H.; Feng, Y.-L. Dichlorobis(pyridinium-2-thiolato)cadmium(II). Acta Crystallogr., Sect. E: Struct. Rep. Online 2005, 61, m767−m768. (c) Wang, X.-J.; Ni, Q.-L.; Shen, Z.-S. Dibromobis[pyridine-2(1H)-thione-κS]cadmium(II). Acta Crystallogr., Sect. E: Struct. Rep. Online 2004, 60, m1918−m1919. (d) Rajalingam, U.; Dean, P. A. W.; Jenkins, H. A. Solution multinuclear (^{31}P, ^{111}Cd, ^{77}Se) magnetic resonance studies of cadmium complexes of heterocyclic aromatic thiones and the structure of [tetrakis(2(1H)-pyridinethione)cadmium] nitrate, [Cd-(C₅H₅NS)₄](NO₃)₂. Can. J. Chem. 2000, 78, 590−597.

(43) Yang, H.; Han, X. L. Syntheses, crystal structures and cleavage mechanism of C-S bond in Cd(II) and Zn(II) complexes with tris(2-mercaptopyridyl)methane. Chinese J. Inorg. Chem. 2015, 31, 1597−1602.

(44) Furthermore, it is longer than the Cd⋯N distances in the 3-trifluoromethyl derivative, Cd(3-CF₃-pyS)₂(bipy), which exhibits a bidentate coordination mode [2.517(2) and 2.576(2) Å]. See: Sousa-Pedrares, A.; Romero, J.; Arturo García-Vázquez, J.; Luz Durán, M.; Casanova, I.; Sousa, A. Electrochemical synthesis and structural characterization of zinc cadmium and mercury complexes of heterocyclic bidentate ligands (N, S). Dalton Trans. 2003, 1379−1388.

(45) Pyridine-2-thiolate ligands may also bridge two metals. For example, see: (a) Wachtler, E.; Gericke, R.; Brendler, E.; Gerke, B.; Langer, T.; Pottgen, R.; Zhechkov, L.; Heine, T.; Wagler, J. Group 10-group 14 metal complexes [E-TM]^{IV}: the role of the group 14 site as an L, X and Z-type ligand. Dalton Trans. 2016, 45, 14252−14264. (b) Deeming, A. J.; Karim, M.; Bates, P. A.; Hursthouse, M. B. A new type of pyridine-2-thionato bridge: X-Ray crystal structure of the complex [Re₂(Mepys)₂(CO)₆] where Mepys is the 6-methylpyridine-2-thionato ligand. Polyhedron 1988, 7, 1401−1403.

(46) For example, see: (a) Wachtler, E.; Gericke, R.; Kutter, S.; Brendler, E.; Wagler, J. Molecular structures of pyridinethiolato complexes of Sn(II), Sn(IV), Ge(IV), and Si(IV). Main Group Met. Chem. 2013, 36, 181−191.

(47) For example, see: Chadwick, S.; Ruhlandt-Senge, K. The remarkable structural diversity of alkali metal pyridine-2-thiolates with mismatched crown ethers. Chem. - Eur. J. 1998, 4, 1768−1780.

(48) (a) Peloquin, D. M.; Schmedake, T. A. Recent advances in hexacoordinate silicon with pyridine-containing ligands: Chemistry and emerging applications. Coord. Chem. Rev. 2016, 323, 107−119. (b) Baus, J. A.; Burschka, C.; Bertermann, R.; Guerra, C. F.; Bickelhaupt, F. M.; Tacke, R. Neutral Six-Coordinate and Cationic Five-Coordinate Silicon(IV) Complexes with Two Bidentate Monoanionic N,S-Pyridine-2-thiolato(−) Ligands. Inorg. Chem. 2013, 52, 10664−10676.

(49) Kedarnath, G.; Jain, V. K. Pyridyl and pyrimidyl chalcogen (Se and Te) compounds: A family of multi utility molecules. Coord. Chem. Rev. 2013, 257, 1409−1435.

(50) (a) Khasnis, D. V. V; Buretea, M.; Emge, T. J.; Brennan, J. G. 2,2′-Bipyridine complexes of the lithium chalcogenolates Li(EPh) and Li(NC₅H₄E-2) (E = S or Se). J. Chem. Soc., Dalton Trans. 1995, 45−48. (b) Kienitz, C. O.; Thone, C.; Jones, P. G. Coordination chemistry of 2,2′-dipyridyl diselenide: X-ray crystal structures of PySeSePy, [Zn-(PySeSePy)Cl₂], [(PySeSePy)Hg(C₆F₅)₂], [Mo(SePy)₂(CO)₃], [W-(SePy)₂(CO)₃], and [Fe(SePy)₂(CO)₂] (PySeSePy = C₅H₄NSeSeC₅H₄N; SePy = [C₅H₄N(2-Se)-N,Se]). Inorg. Chem. 1996, 35, 3990−3997. (c) Chopra, N.; Damude, L. C.; Dean, P. A. W.; Vittal, J. J. Pyridine-2-selenolate and −2-tellurolate as ligands: a multinuclear (^{77}Se, ^{119}Sn, ^{125}Te) magnetic resonance study of some tin(IV) complexes, and X-ray structural analyses of Sn(SPh)₂(2-Se-C₅H₄N-N,Se)₂ and Sn(SPh)₁.₈₅(2-Se-C₅H₄N)₂.₁₅. Can. J. Chem. 1996, 74, 2095−2105. (d) Narayan, S.; Jain, V. K.; Varghese, B. Pyridine-2-selenolate complexes of palladium(II) and platinum(II): crystal structure of [(Prⁿ₃P)Cl₂Pd(NC₅H₄Se)PdCl(PPrⁿ₃)]. J. Chem. Soc., Dalton Trans. 1998, 2359−2366. (e) Rong, Y.; Parkin, G. The synthesis and structures of tris(2-pyridylseleno)methyl zinc compounds with κ²-, κ³-, and κ⁴-coordination modes. Aust. J. Chem. 2013, 66, 1306−1310. (f) Cheng, Y. F.; Emge, T. J.; Brennan, J. G. Pyridineselenolate complexes of tin and lead: Sn(2-SeNC₅H₄)₂, Sn(2-SeNC₅H₄)₄, Pb(2-SeNC₅H₄)₂, and Pb(3-Me₃Si-2-SeNC₅H₃)₂. Volatile CVD precursors to group IV group VI

semiconductors. Inorg. Chem. 1996, 35, 342−346. (g) Sharma, R. K.; Kedarnath, G.; Wadawale, A.; Betty, C. A.; Vishwanadh, B.; Jain, V. K. Diorganotin(IV) 2-pyridyl selenolates: synthesis, structures and their utility as molecular precursors for the preparation of tin selenide nanocrystals and thin films. Dalton Trans. 2012, 41, 12129−12138. (h) Sharma, R. K.; Kedarnath, G.; Jain, V. K.; Wadawale, A.; Pillai, C. G. S.; Nalliath, M.; Vishwanadh, B. Copper(I) 2-pyridyl selenolates and tellurolates: Synthesis, structures and their utility as molecular precursors for the preparation of copper chalcogenide nanocrystals and thin films. Dalton Trans. 2011, 40, 9194−9201.

(51) (a) Cheng, Y. F.; Emge, T. J.; Brennan, J. G. Polymeric Cd(Se-2-NC₅H₄)₂ and square-planar Hg(Se-2-NC₅H₄)₂ - Volatile CVD precursors to II-VI semiconductors. Inorg. Chem. 1994, 33, 3711−3714. (b) Sharma, R. K.; Kedarnath, G.; Wadawale, A.; Jain, V. K.; Vishwanadh, B. Monomeric pyridyl-2-selenolate complexes of cadmium and mercury: Synthesis, characterization and their conversion to metal selenide nanoparticles. Inorg. Chim. Acta 2011, 365, 333−339.

(52) The Cd−Se bond length of [Tm$^{Bu^t}$]CdSePy is also comparable to that of [Tm$^{Bu^t}$]CdSePh [2.5595(5) Å]. See ref 24.

(53) The longer Cd⋯N distance for [Tm$^{Bu^t}$]CdSPy is consistent with the slightly larger angle at selenium [93.32(5)°] than at sulfur [91.95(10)°].

(54) Bergquist, C.; Storrie, H.; Koutcher, L.; Bridgewater, B. M.; Friesner, R. A.; Parkin, G. Factors influencing the thermodynamics of zinc alkoxide formation by alcoholysis of the terminal hydroxide complex, [Tp$^{Bu^t,Me}$]ZnOH: An experimental and theoretical study relevant to the mechanism of action of liver alcohol dehydrogenase. J. Am. Chem. Soc. 2000, 122, 12651−12658.

(55) For substituent effects on ArS−H bond dissociation energies, see: (a) Bordwell, F. G.; Zhang, X. M.; Satish, A. V.; Cheng, J. P. Assessment of the importance of changes in ground-state energies on the bond-dissociation enthalpies of the O−H bonds in phenols and the S−H Bonds in thiophenols. J. Am. Chem. Soc. 1994, 116, 6605−6610. (b) Borges dos Santos, R. M.; Martinho Simões, J. A. Energetics of the O−H bond in phenol and substituted phenols: A critical evaluation of literature data. J. Phys. Chem. Ref. Data 1998, 27, 707−739. (c) Borges dos Santos, R. M.; Muralha, V. S. F.; Correia, C. F.; Guedes, R. C.; Costa Cabral, B. J.; Martinho Simões, J. A. S−H bond dissociation enthalpies in thiophenols: A time-resolved photoacoustic calorimetry and quantum chemistry study. J. Phys. Chem. A 2002, 106, 9883−9889. (d) Kuznetsova, O. V.; Egorochkin, A. N.; Khamaletdinova, N. M.; Domratcheva-Lvova, L. G. Bond dissociation energies in organometallic systems: substituent effects. J. Phys. Org. Chem. 2014, 27, 850−859. (e) Fu, Y.; Lin, B. L.; Song, K. S.; Liu, L.; Guo, Q. X. Substituent effects on the S−H bond dissociation energies of thiophenols. J. Chem. Soc. Perkin Trans. 2 2002, 1223−1230. (f) Rimarcik, J.; Lukes, V.; Klein, E.; Rottmannova, L. On the enthalpies of homolytic and heterolytic S−H bond cleavage in para and meta substituted thiophenols. Comput. Theor. Chem. 2011, 967, 273−283.

(56) For other examples of electron-withdrawing substituents increasing M−SAr homolytic bond dissociation energies, see: (a) Zeng, Q.; Li, Z.; Wang, Y.; Zhai, H.; Tao, O.; Wang, Y.; Guan, J.; Zhang, Y. Substituent effects on gas-phase homolytic Fe-O and Fe-S bond energies of m-G-C₆H₄OFe(CO)₂(η⁵-C₅H₅) and m-G-C₆H₄SFe-(CO)₂(η⁵-C₅H₅) studied using Hartree-Fock and density functional theory methods. J. Phys. Org. Chem. 2016, 29, 172−184. (b) Zeng, Q.; Li, Z.; Dong, L.; Han, D.; Wang, R.; Li, X.; Bai, G. Remote substituent effects on gas-phase homolytic Fe-O and Fe-S bond energies of p-G-C₆H₄OFe(CO)₂(η⁵-C₅H₅) and p-G-C₆H₄SFe(CO)₂(η⁵-C₅H₅) studied using Hartree-Fock and density functional theory methods. J. Phys. Org. Chem. 2013, 26, 664−674. (c) Zhang, J.; Adhikary, A.; King, K. M.; Krause, J. A.; Guan, H. R. Substituent effects on Ni−S bond dissociation energies and kinetic stability of nickel arylthiolate complexes supported by a bis(phosphinite)-based pincer ligand. Dalton Trans. 2012, 41, 7959−7968.

(57) Electron-withdrawing substituents decrease both M−SAr and M−SH heterolytic bond dissociation energies because the substituents stabilize the ArS⁻ anion to a greater extent than they do the respective

neutral molecules; however, the effect is expected to be smaller for the M−SAr bond because it is more polar than the H−SAr bond.

(58) For another example of electron-withdrawing substituents decreasing M−SAr heterolytic bond dissociation energies, see: Zeng, Q.; Li, Z.; Han, D.; Dong, L.; Zhai, H.; Liu, B.; Bai, G.; Zhang, Y. Hartree-Fock and density functional theory study of remote substituent effects on gas-phase heterolytic Fe-O and Fe-S bond energies of p-G-$C_6H_4OFe(CO)_2(\eta^5$-$C_5H_5)$ and p-G-$C_6H_4SFe(CO)_2(\eta^5$-$C_5H_5)$. *J. Phys. Org. Chem.* **2014**, *27*, 142−155.

(59) For the effect of electron-donating and electron-withdrawing substituents on heterolytic bond dissociation energies and pK_a values, see ref 55f and: Hunter, N. E.; Seybold, P. G. Theoretical estimation of the aqueous pK_as of thiols. *Mol. Phys.* **2014**, *112*, 340−348.

(60) (a) Bain, A. D. Chemical exchange. *Annu. Rep. NMR Spectrosc.* **2008**, *63*, 23−48. (b) Bain, A. D. Chemical exchange in NMR. *Prog. Nucl. Magn. Reson. Spectrosc.* **2003**, *43*, 63−103. (c) Perrin, C. L.; Dwyer, T. J. Application of 2-dimensional NMR to kinetics of chemical exchange. *Chem. Rev.* **1990**, *90*, 935−967. (d) Dimitrov, V. S.; Vassilev, N. G. Dynamic NMR: A new procedure for the estimation of mixing times in the 2D EXSY experiments. A four-site exchange system studied by 1D and 2D EXSY spectroscopy. *Magn. Reson. Chem.* **1995**, *33*, 739−744.

(61) Note that the ^{19}F line width of $[Tm^{Bu^t}]CdSC_6H_4$-4-F in the absence of exchange is larger than that for HSC_6H_4-4-F.

(62) (a) McNally, J. P.; Leong, V. S.; Cooper, N. J. Cannula techniques for the manipulation of air-sensitive materials. In *Experimental Organometallic Chemistry*; Wayda, A. L., Darensbourg, M. Y., Eds.; American Chemical Society: Washington, DC, 1987; Chapter 2, pp 6−23. (b) Burger, B. J.; Bercaw, J. E. Vacuum line techniques for handling air-sensitive organometallic compounds. In *Experimental Organometallic Chemistry*; Wayda, A. L., Darensbourg, M. Y., Eds.; American Chemical Society: Washington, DC, 1987; Chapter 4, pp 79−98. (c) Shriver, D. F.; Drezdzon, M. A. *The Manipulation of Air-Sensitive Compounds*, 2nd ed.; Wiley-Interscience: New York, 1986.

(63) Fulmer, G. R.; Miller, A. J. M.; Sherden, N. H.; Gottlieb, H. E.; Nudelman, A.; Stoltz, B. M.; Bercaw, J. E.; Goldberg, K. I. NMR chemical shifts of trace impurities: Common laboratory solvents, organics, and gases in deuterated solvents relevant to the organometallic chemist. *Organometallics* **2010**, *29*, 2176−2179.

(64) Dungan, C. H.; van Wazer, J. R. *Compilation of Reported ^{19}F NMR Chemical Shifts 1951 to mid 1967*; Wiley-Interscience: New York, 1970.

(65) Laube, J.; Jäger, S.; Thöne, C. Synthesis and Structural Studies of Pyridine-2-selenolates − Reactions with Electrophilic Phosphorus(III) Compounds and Related Complex Chemistry. *Eur. J. Inorg. Chem.* **2001**, *2001*, 1983−1992.

(66) (a) Sheldrick, G. M. *SHELXTL, An Integrated System for Solving, Refining, and Displaying Crystal Structures from Diffraction Data*; University of Göttingen: Göttingen, Germany, 1981. (b) Sheldrick, G. M. A short history of SHELX. *Acta Crystallogr., Sect. A: Found. Crystallogr.* **2008**, *64*, 112−122.